

# Paper Synopsis

Xiaoyin Zhu  
Nov 5, 2012  
OPTI 521

**Paper: Active Optics and Wavefront Sensing at the Upgraded 6.5-meter MMT** by T. E. Pickering, S. C. West, and D. G. Fabricant

**Abstract:** This synopsis summarized the key information of the paper “Active Optics and Wavefront Sensing at the Upgraded 6.5-meter MMT”. In the paper, two Shack-Hartmann wavefront sensors that used at both of the optical foci (f/9 and f/5) of the converted MMT were described. How the two systems have performed thus far is also covered in the paper.

## 1. Introduction

In order to get excellent images, the wavefront error need to be measured and corrected, especially for borosilicate mirrors, such as the 6.5-meter MMT primary, because they can be distorted by temperature gradients. Shack-Hartmann wavefront sensors are a common and powerful tool for measuring wavefront error in optical systems. In addition to the adaptive f/15 system, the MMT has two other operational foci: an f/9 system designed for compatibility with preconversion MMT instruments and a wide-field f/5 system capable of providing highly corrected images over fields  $0.5^\circ$  diameter in imaging mode and  $1.0^\circ$  diameter in spectroscopic mode. Shack-Hartmann wavefront sensors for both of these foci have been commissioned and put into routine use over the past year.

## 2. F/9 wavefront sensor

Figure 1 shows a labeled picture of the completed instrument before its installation in the f/9 top box. The whole assembly is mounted on a two-axis motorized slide with one axis used to adjust focus and the other to select between wavefront sensor and direct imaging optics. The wavefront sensor optics consist of a 45 mm focal length 13x13 hexagonal geometry lenslet array, an 80 mm focal length collimator lens, and an RG610 blue cutoff filter. The camera is an Apogee KX-260 CCD (512x512 with 20 micron pixels and 14-bit readout). The effective wavelength of the filter plus CCD is 7800 Å and in practice a 9th magnitude K star can saturate the camera within 30 seconds in good seeing. Example reference and data images taken with the system are shown in Figure 2.

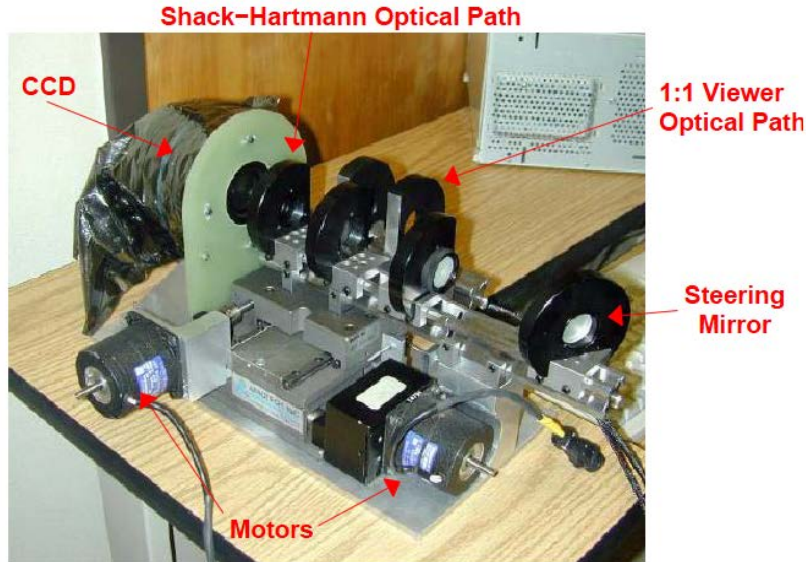


Figure 1. The as-built f/9 Shack-Hartmann device prior to installation in the top box.

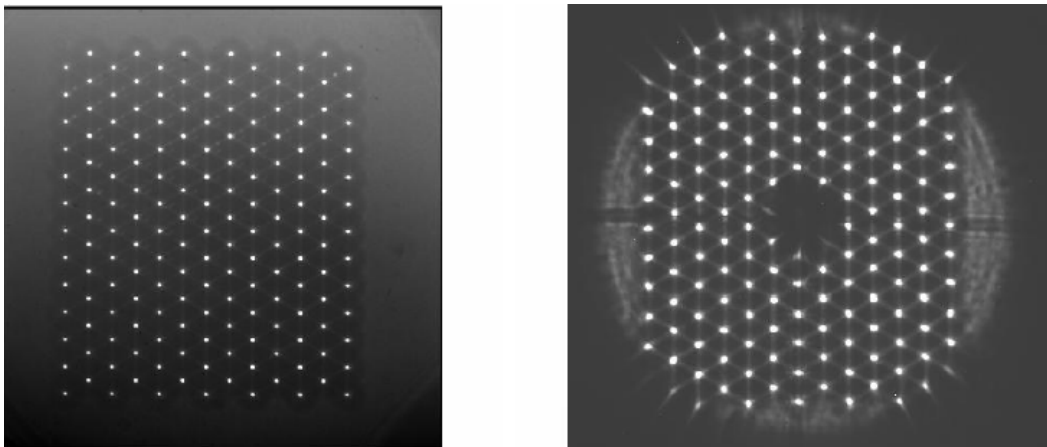


Figure 2. Representative reference (left) and data (right) images taken with the f/9 Shack-Hartmann wavefront sensor.

### 3. F/5 wavefront sensor

The f/5 wavefront sensor system consists of a commercial Shack-Hartmann wavefront sensor and a separate CCD camera with a filter wheel that can be used for time-critical imaging while a spectroscopic instrument is mounted at the f/5 focus. The wavefront sensor used is a slightly modified Puntino unit from Spot Optics. A negative field lens is added to image the system pupil on the lenslet array, and the original 0.3 mm pitch lenslet array is replaced with a coarser 0.6 mm lenslet array (14x14 samples across the pupil). The collimator and lenslet array focal lengths are both 40 mm. The wavefront sensor camera is a SBIG ST9XE (512x512 with 20  $\mu\text{m}$  pixels). A beamsplitter sends half of the light to the wavefront sensor and the other half to an acquisition camera, a Pixelink PL-A641. The direct imaging CCD camera is an Apogee AP8p that contains a thinned 1024x1024 chip with 24  $\mu\text{m}$  pixels (about 0.14"/pixel). Figure 3 is a drawing of the f/5 wavefront sensor system. Figure 4 shows representative reference and data images.

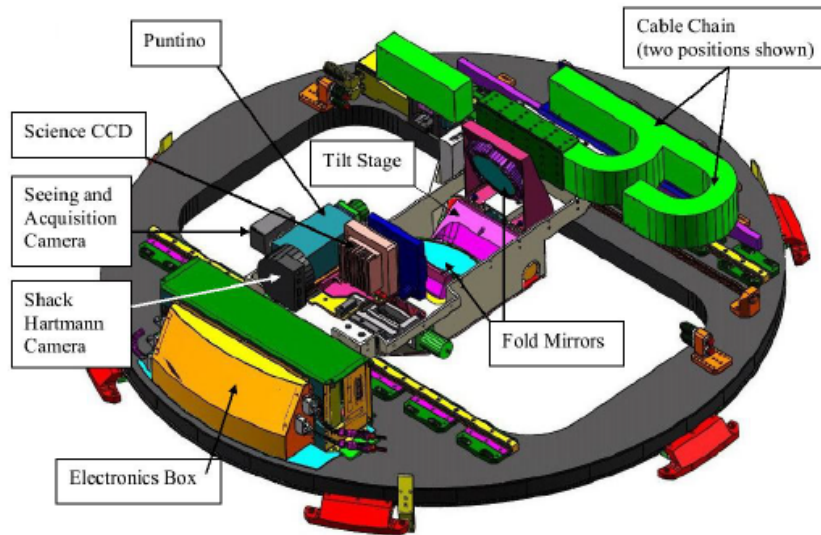


Figure 3. Drawing of the f/5 wavefront sensor package with its cover removed.

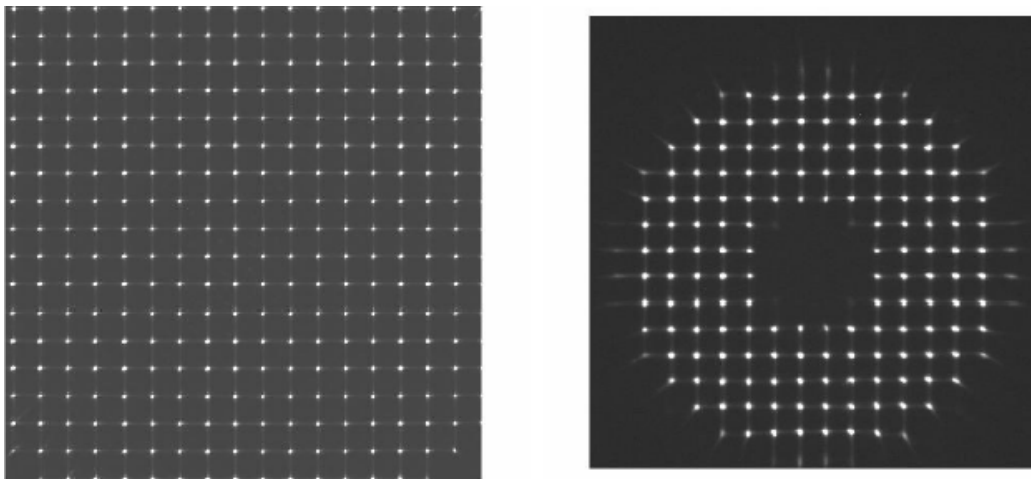


Figure 4. Representative reference (left) and data (right) images taken with the f/5 wavefront sensor.

#### 4. Wavefront analysis and software

The two wavefront sensors share a common software interface that fits a set of 19 Zernike polynomials to the wavefront errors. Zernike focus and coma are corrected by moving the secondary mirror, third order spherical by a combination of secondary motion and primary bending, and the rest by primary bending alone. The software used to control the wavefront sensors and analyze the acquired data is a modular mixture of IRAF and custom C code glued together with perl, TCL, and ruby scripts. Wavefront slopes are calculated from the spot displacements and modeled with a 19-term Zernike polynomial fit. The resulting fit is displayed in the form of a pupil phase map, an image point-spread function map, and a bar graph showing the RMS wavefront error contributions of each Zernike component.

## 5. Results and performance

Table 1 summarizes the average beginning of night wavefront measurements for the f/9 and f/5 wavefront sensors, giving an indication of the telescope's initial condition before wavefront correction. Table 2 tabulates averages of wavefront measurements taken after corrections have been completed. In general these consist of two or three corrective iterations. The averages for the lower order terms are all much smaller than at the beginning of the night.

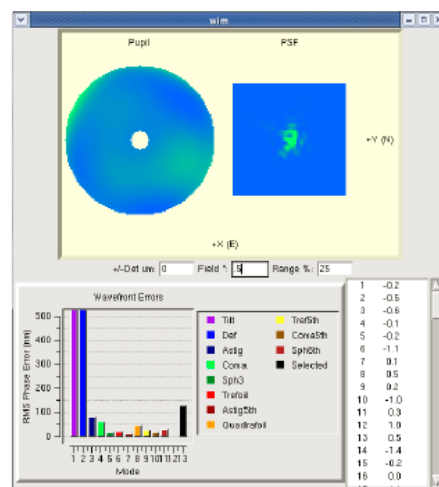
Table 1 Data before correction.

Zernike Mode	F/5 (nm)	F/9 (nm)
Astigmatism (45°)	467 ± 478	576 ± 591
Astigmatism (0°)	-494 ± 770	354 ± 1089
X Coma	458 ± 1726	87 ± 1233
Y Coma	327 ± 1266	61 ± 823
3rd Order Spherical	-91 ± 596	491 ± 545
X Trefoil	417 ± 306	456 ± 331
Y Trefoil	-179 ± 284	-21 ± 242
5th Order Astigmatism (45°)	-44 ± 205	-326 ± 228
5th Order Astigmatism (0°)	17 ± 228	-226 ± 267
Quadrafoil 1	146 ± 143	-46 ± 191
Quadrafoil 2	-81 ± 208	165 ± 287
5th Order X Trefoil	-85 ± 143	-174 ± 189
5th Order Y Trefoil	-45 ± 122	55 ± 110
5th Order X Coma	42 ± 254	-183 ± 215
5th Order Y Coma	-57 ± 163	-103 ± 188
6th Order Spherical	4 ± 191	-83 ± 194

Table 2 Data after correction.

Zernike Mode	F/5 (nm)	F/9 (nm)
Astigmatism (45°)	-4 ± 376	3 ± 412
Astigmatism (0°)	-19 ± 393	28 ± 440
X Coma	-9 ± 187	-28 ± 253
Y Coma	9 ± 221	-14 ± 292
3rd Order Spherical	-78 ± 205	-15 ± 133
X Trefoil	58 ± 187	20 ± 203
Y Trefoil	22 ± 192	-44 ± 257
5th Order Astigmatism (45°)	-21 ± 129	-135 ± 245
5th Order Astigmatism (0°)	48 ± 224	-38 ± 230
Quadrafoil 1	123 ± 119	80 ± 178
Quadrafoil 2	-103 ± 142	27 ± 203
5th Order X Trefoil	-46 ± 133	-146 ± 170
5th Order Y Trefoil	-46 ± 94	-4 ± 108
5th Order X Coma	-33 ± 163	-159 ± 160
5th Order Y Coma	-59 ± 98	-74 ± 132
6th Order Spherical	-18 ± 176	18 ± 167

Figure 7 shows a representative example of how well the MMT optics can be tuned when the conditions are good. The seeing was exceptionally good (0.25–0.3") at this time, so the high order modes were corrected. The enclosed energy fraction within a 0.1" radius is 82% for the Zernike fit versus 47% calculated directly from the spot motions. Part of this difference is due to centroiding uncertainty since the RMS spot deviation of 0.106" corresponds to 0.014 pixels.



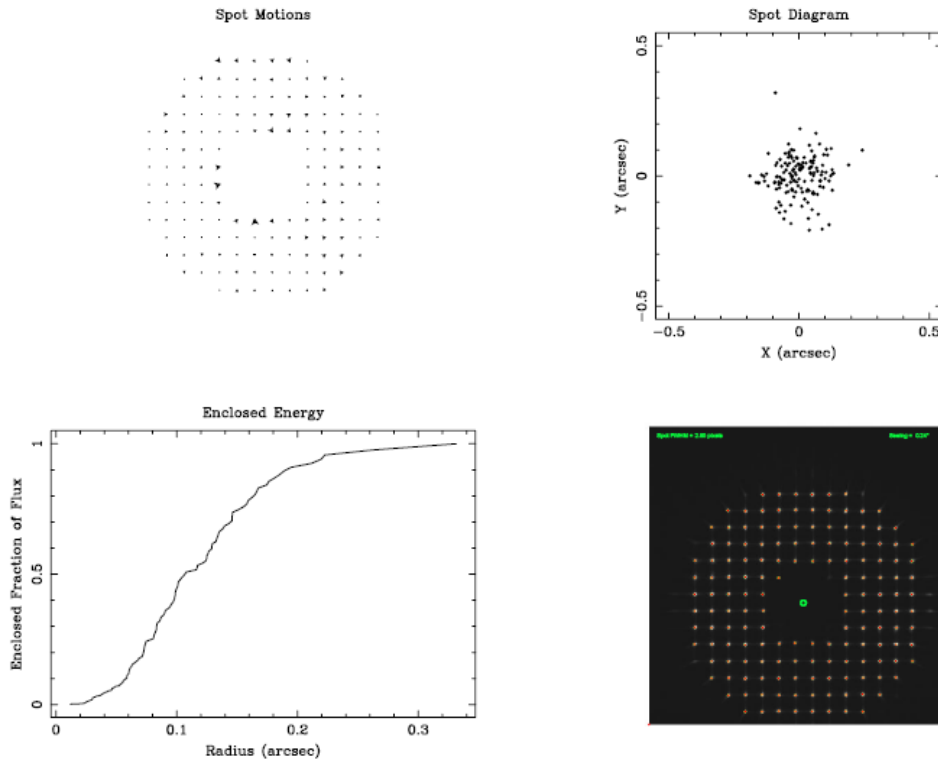


Figure 7. Screenshot of Zernike polynomial fit (top) and spot motion analysis (bottom) of wavefront performance on a very good night after wavefront corrections have been applied. The Shack-Hartmann data was taken at an elevation of  $85^\circ$  in  $0.25\text{--}0.3''$  seeing with a total exposure time of 20 seconds. The RMS spot deviation is  $0.106''$ .

Without the benefit of continuous wavefront monitoring, the ability to maintain telescope performance between rounds of wavefront sensing is at least as important as the performance of the wavefront sensors themselves. The largest factors that must be dealt with are gravity and the temperature of the optical support structure (OSS) of the telescope. The effect of gravity is calibrated by taking wavefront sensor data over a range of elevation Angles. Correcting for OSS temperature changes should in principle be quite easy, and the thermal expansion of the borosilicate primary mirror is also well-determined. Keeping the primary and f/9 secondary mirrors isothermal is another important component of maintaining good image quality.

## 6. Conclusions and future work

The wavefront sensor systems of MMT have worked very well so far and have significantly enhanced the overall performance and productivity of the telescope. However, some significant improvements are still need to be made: the telescope operator interface; open-loop performance; open-loop handling of elevation-dependent; and the open-loop corrections of the primary as well.

## References

Active Optics and Wavefront Sensing at the Upgraded 6.5-meter MMT by T. E. Pickering, S. C. West, and D. G. Fabricant